Pergamon

Geochimica et Cosmochimica Acta, Vol. 66, No. 12, pp. 2139–2153, 2002

0016-7037/02 $22.00 + .00

PII S0016-7037(02)00898-0

Generation and differentiation of group II kimberlites: Constraints from a high-pressure experimental study to 10 GPa

PETER ULMER* and RUSSELL J. SWEENEY[1]
Department of Earth Sciences, ETH-Zentrum, CH-8092, Zurich, Switzerland

(*Received June* 25, 2001; *accepted in revised form March* 11, 2002)

Abstract—Experiments have been performed in the multicomponent (natural) bulk system to constrain the conditions of generation and differentiation of a K-rich group II kimberlite (now also referred to as orangeite). The group II composition examined was saturated in olivine, orthopyroxene, and garnet at near liquidus conditions in the pressure range 4 to 10 GPa. In the range 2 to 3 GPa, the liquidus phase was olivine only. The potassic nature of the melts in the bulk compositions studied was ensured by the absence of any K-bearing phase in the residual assemblage at $P > 4$ GPa. Phlogopite is destabilized toward higher pressures by a carbonation reaction of the type phlogopite + CO_2 = enstatite + garnet + K_2CO_3 (liquid) + H_2O leading to alkalic, carbonatitic liquids coexisting with a garnet–peridotite (harzburgite or lherzolite) residue over a wide pressure–temperature space at pressures in excess of 4 GPa. Evidently, CO_2-bearing systems do not favor the stability of phlogopite and/or K-richterite amphibole at pressures in excess of 4 to 5 GPa, and it is suggested that the carbonate-bearing and potassic character of any mantle melt originating from this depth is most likely the product of a two-stage process: either a carbonate-bearing protolith is invaded by a potassic melt or fluid (probably supercritical), or a potassic protolith (after metasomatism) has been invaded by a carbonatite melt. *Copyright © 2002 Elsevier Science Ltd*

1. INTRODUCTION

Kimberlites, CO_2-rich ultrabasic silicate magmas, are one of the main magmas by which diamonds are brought to the Earth's surface, and consequently, they have attracted much attention as deep probes into the mantle. Currently, two models exist for the origin of kimberlites: first, by the small degree partial melting of a carbonated lherzolite (e.g., Dawson, 1980; Mitchell, 1986, 1995; Eggler, 1989; Canil and Scarfe, 1990; Tainton and McKenzie, 1994; Dalton and Presnall, 1998b) or second, by production from the interaction of volatiles migrating from depth with shallower mantle (Wyllie, 1980, 1989; Green et al., 1987) and reviewed in Wyllie, 1994). In either event, equilibrium should exist between any small-volume melts and the source mineralogy, regardless of the mode of origin. Therefore, the determination of a condition where a kimberlitic melt saturates in mantle phases just below its liquidus provides information on conditions of origin. This is the rationale of many previous experimental studies that have examined kimberlitic phase relations (Eggler and Wendlandt, 1979; Edgar et al., 1988; Ringwood et al., 1992; Edgar and Charbonneau, 1993; Girnis et al., 1995; Yamashita et al., 1995).

Smith et al. (1985) divided kimberlites into group I (basaltic) and group II types (micaceous, now called orangeites by Mitchell, 1995) on the basis of their geochemistry, and concluded the former to be asthenospheric and the latter to be mantle lithospheric derived. All but one previous experimental study of kimberlite phase relations have been carried out on group I bulk compositions; the only exception is the study of Yamashita et al. (1995) on an aphanitic and macrocrystic group II kimberlite from the Makganyene Mine, South Africa. Here, we choose a bulk composition that is representative of a potassic (group II) kimberlite.

The primary aim of this work is to examine kimberlite origins by investigating its high-pressure phase equilibria and to evaluate them in the context of other volatile-rich mantle samples, such as carbonatites and hydrous mantle xenoliths, which represent a spectrum of small-degree mantle melts or fluids (e.g., MARIDs, or mica–amphibole–rutile–ilmenite–diopside suite of mantle xenoliths; Dawson and Smith, 1977). MARIDs and K-rich carbonatites might represent products of "failed" kimberlites. Close association of K-rich micaceous group II kimberlites and MARIDs have been proposed repeatedly on the bases of (1) regional distribution of MARIDs and group II kimberlites, restricted exclusively to the Kaapvaal Craton (Mitchell, 1995), (2) geochemistry (major, trace and isotope geochemistry reveals strong similarities between MARID-type xenoliths and micaceous, group II kimberlites, e.g., Jones, 1989), and (3) overlapping ages of group II kimberlites and MARIDs in the range 110 to 150 myr (Konzett et al., 1998). Straightforward mass-balance constraints (Sweeney et al., 1993) indicate that the carbonate-free MARIDs can only be derived from a group II kimberlite liquid through differentiation and/or reaction processes with the surrounding peridotite if a (K-rich) carbonatite component has been produced concomitantly with the MARID phase assemblage.

Here we present experimental phase equilibria and analytical data on an (average) K-rich micaceous group II kimberlite to constrain its generation from metasomatized peridotitic mantle and to evaluate its differentiation products at mantle (lithospheric) mantle conditions. The selected starting composition (Table 1, labeled A) corresponds closely to the average group II kimberlite reported by Smith et al. (1985), except for a higher Na_2O content (0.93 instead of 0.10) to explore Na-K relation-

* Author to whom correspondence should be addressed (peter.ulmer@erdw.ethz.ch).
[1] *Present address:* De Beers GeoScience Centre, P.O. Box 82232, Southdale 2135, South Africa.

Table 1. Kimberlite bulk composition used in this study and past experimental studies[a].

Element	A GPII	MARID AJE137	GP Ia[b]	GP Ib[b]	GP II[b]	EW[c]	Edgar[c]	Ringwood[c]	Girnis[c]	YAO[c]	S94
SiO_2	35.48	49.94	32.10	25.70	36.30	37.68	25.60	33.80	36.9	39.10	8.16
TiO_2	1.00	3.13	2.00	3.00	1.00	2.16	3.35	2.10	1.96	1.02	0.69
Cr_2O_3	0.30	0.16				0.23			0.20		0.08
Al_2O_3	3.16	6.78	2.60	3.10	3.20	t5.11	3.31	3.60	3.50	3.05	1.56
FeO	8.22	6.98	8.30	11.42	7.60	11.27	9.26	8.00	10.3	8.38	4.07
MnO	0.24	0.07	0.20	0.20	0.20		0.21				
MgO	29.10	21.72	28.50	23.80	29.70	25.85	27.20	31.50	36.0	30.20	13.93
NiO	0.44	0.11									
CaO	5.88	5.91	8.20	14.10	6.00	10.62	15.30	8.10	8.95	6.18	21.91
Na_2O	0.93	0.99	0.20	0.20	.10	0.22	0.28	0.40	0.20	0.17	2.10
K_2O	3.17	7.21	1.10	0.60	3.20	0.91	0.70	1.10	1.00	3.55	5.35
P_2O_5	0.00	0.00	1.10	1.10	1.10	0.00	1.83	1.30	1.00	0.79	0.00
CO_2	7.13		4.60	8.60	3.60	5.22	4.77	5.00	31–10	4.37	
H_2O	4.97		10.60	8.98	6.80	5.00	6.20	5.30	0–11	3.31	
Total	100.02	100.00	99.50	100.80	98.80	99.27	99.05	100.20	100.01	100.12	57.85
x_{Mg}	0.863	0.847	0.860	0.788	0.874	0.803	0.840	0.875	0.862	0.865	0.859
CS	0.201		0.143	0.3335	0.100	0.139	0.186	0.148	0.84–0.27	0.112	
x_{CO_2}	0.370	0.000	0.151	0.281	0.178	0.299	0.240	0.278	0.34–1.00	0.3551	

[a] GPII = group II kimberlite; MAR1D = AJE137 composition used by Sweeney et al. (1993); GP Ia = group Ia Kimberlite average (Smith et al., 1985); GP Ib = group Ib kimberlite average (Smith et al., 1985); GP II = group II = kimberlite average (Smith et al., 1985); EW = Lesotho kimberlite (Eggler and Wendlandt, 1979), using Co as Fe analog; Edgar = aphanitic kimberlite from Wesselton (Edgar et al., 1988) Ringwood = group I composition from Ringwood et al. (1992), Fe as Co; Girnis = group Ia composition from Girnis et al. (1995); YAO = group; Makganyene kimberlite from Yamashita et al. (1995); S94 = Sweeney (1994), primary carbonatite at 3.4 GPa and 1100°C. Total Fe is reported as FeO. x_{Mg} = molar ratio of MgO/(MgO + FeO); CS = CO_2/SiO_2 (wt%); x_{CO_2} = molar ration of $CO_2/(CO_2 + H_2O)$.

[b] Kimberlite average.

[c] Kimberlite.

ships and a higher CO_2 and lower H_2O content resulting in about twice the x_{CO_2} (0.37 instead of 0.18) of the average group II kimberlite reported by Smith et al. (1985). The adjustment of the volatile components was mainly guided by the mass-balance considerations of Sweeney et al. (1993). To what extend these adjustments influenced the results of the phase equilibrium study is addressed in sections 3.1 and 4, where the data are presented and discussed.

2. EXPERIMENTAL AND ANALYTICAL TECHNIQUES

2.1. Starting Materials

The starting composition of the group II kimberlite listed in Table 1 (A) was synthesized from reagent-grade chemicals, previously dried at 1100°C (SiO_2, TiO_2, Cr_2O_3, Al_2O_3, MgO, MnO, NiO), weighed, homogenized in an agate mortar under alcohol, and fired again at 1100°C. Fe was added as presynthesized fayalite, and carbonate was added as $CaCO_3$, K_2CO_3, Na_2CO_3, and $MgCO_3$. H_2O (5 wt%) was either added by microsyringe (±0.5 wt% accuracy) or as $Mg(OH)_2$. Compositions were homogenized, dried, and stored at 120°C in a vacuum furnace. Most runs were carried out in 2.3- and 1.6-mm outer diameter sealed $Ag_{50}Pd_{50}$ or $Ag_{25}Pd_{75}$ capsules. Initially, high-temperature experiments (≥1350°C; Table 2) have been performed in Pt capsules. Pt containers are known to be problematic in Fe-bearing systems as a result of Fe loss resulting from alloying with the Pt capsule that in turn leads to oxidation and hydrogen loss in hydrous experiments. To minimize Fe loss to the Pt capsules, run times were kept short at high temperatures (0.1 to 0.5 h at temperature ≥1350°C). An additional reason to keep run times short is the observation that alkali–carbonate liquids are corrosive against the noble metal containers and dissolve them in short time. Subsequently, we conducted a series of additional experiments (Table 2) by means of graphite liners containing the starting material (1.4 mm OD, 0.8 mm ID, 1.4 mm long, tightly packed graphite powder at the bottom and top) that were sealed in 1.6-mm outer diameter Pt capsules. These later experiments were used to constrain fO_2 (on the graphite/diamond −COH equilibrium) and to test the influence of Fe loss observed on the phase equilibria in the highest temperature runs with Pt capsules. Comparison of the phase equilibria and mineral data, in particular the forsterite content of olivine obtained from AgPd/Pt experiments and graphite-lined experiments at 7.5 and 8.0 GPa, suggests that Fe loss to Pt crucibles was not excessive (with two exceptions) and that the phase equilibria are not seriously affected by this problem.

2.2. Piston Cylinder Apparatus

Up to 3.5 GPa, an end-loaded piston cylinder with a 14-mm bore was used. NaCl-Pyrex assemblies were used to the highest temperatures. Temperatures were measured with Pt-$Pt_{90}Rh_{10}$ thermocouples and are considered to be accurate to ±10°C, without taking into account the effect of pressure on the emf. Pressure was calibrated at 1000°C against the reaction fayalite + quartz = orthoferrosilite (1.41 GPa; Bohlen and Boettcher, 1982) and the quartz–coesite transition (3.07 GPa; Bose and Ganguly, 1995). Pressures are considered to be accurate to ±0.1 GPa.

2.3. Multianvil Apparatus

All experiments at pressure >3.5 GPa were performed in a Walker-type multianvil apparatus (Walker et al., 1990; Walker, 1991). The multianvil experiments summarized in Table 2 have been performed with WC cubes with truncated edge lengths of 12 mm. The pressure transmitting octahedron and gasket fins were fabricated from MgO-based castable ceramics (Ceramcast 584). All runs were performed with 4.5- and 3.5-mm outer diameter graphite furnace assemblies. Stepped graphite heaters were used to minimize thermal gradients. Temperatures were measured with Pt-$Pt_{90}Rh_{10}$ and W_5Re-$W_{26}Re$ thermocouples. The thermal gradient at 1200°C did not exceed 20°C per mm (for details of assembly and measurement of thermal gradients, see Konzett et al., 1997). This is supported by the lack of significant variation of the amount of melt (relative to crystals) and/or the composition of solid phases (e.g., coexisting clinopyroxene–orthopyroxene) between the center and the top or bottom end of the capsule. The thermal gradient calculated with the two-pyroxene thermometer of Brey and Koehler (1990) was found to be less than 45°C over 1.6 mm

Table 2. Run conditions and results of kimberlite high-pressure melting experiments[a].

Run	T (°C)	P (GPa)	Time (hr)	Technique	Product phases	x_{Mg} Ol
472	1200	1.5	2.7	PC	ol L	ND
470	1150	2.0	6.0	PC	ol cpx phl L	0.892
468	1200	2.0	2.7	PC	ol phl L	0.948
469	1200	2.5	2.6	PC	ol cpx phl sp L	0.882
474	1250	2.5	2.5	PC	ol cpx opx phl L	0.898
542	1300	2.5	0.8	PC	ol (phl) L	0.900
471	1200	3.0	2.5	PC	ol gar cpx phl L	ND
473	1250	3.0	2.7	PC	ol opx phl L	0.920
541	1300	3.0	0.9	PC	ol opx (phl) L	0.906
543	1150	3.8	2.0	MA	ol cpx opx phl L	0.901
540	1200	3.8	0.2	MA	ol gar cpx opx L	0.895
547[b]	1350	4.0	0.5	MA	ol opx L	0.957
MA27	1150	4.6	1.5	MA	ol gar opx cpx usp L	0.898
MA26	1250	4.6	1.0	MA	ol gar opx L	0.898
MA28[b]	1400	4.6	0.3	MA	ol opx L	0.937
MA21	1250	6.0	0.5	MA	ol gar opx L	0.895
MA20[b]	1350	6.0	0.1	MA	ol gar opx L	0.914
525[b]	1400	6.0	0.5	MA	ol gar opx L	0.928
548[b]	1480	6.0	0.2	MA	ol gar opx L	0.945
MA24	1150	7.5	0.7	MA	ol gar opx cpx mag ilm L	0.897
MA25	1200	7.5	0.5	MA	ol gar opx cpx L	0.903
MA22	1280	7.5	0.3	MA	ol gar opx L	0.909
MA23	1300	7.5	0.5	MA	ol gar opx L	0.909
524[b]	1450	7.5	0.3	MA	ol gar opx L	0.926
561	900	8.0	20.0	MA	cpx opx gar mag L	
642[c]	1200	8.0	23.0	MA	ol gar opx cpx mag rut LL	0.888
646[c]	1500	8.0	1.0	MA	ol gar opx L	0.925
652[c]	1200	9.5	2.0	MA	ol gar opx cpx mag L	0.881
653[c]	1400	9.5	1.0	MA	ol gar opx L	0.910
655[c]	1600	9.5	0.5	MA	ol gar opx L	0.921

[a] Technique indicates experimental technique used: PC = piston-cylinder; MA = multianvil apparatus. Phases: ol = olivine; cpx = clinopyroxene (high-Ca pyroxene); opx = orthopyroxene (low-Ca pyroxene); gar = garnet; phl = phlogopite; sp = Cr-spinel; L = liquid phase (quench); usp = ulvöspinel; ilm = ilmenite; rut = TiO_2 (α-PbO_2 structure verified by Micro-Raman spectroscopy); mag = magnesite. Product phases in parentheses indicate quench products. x_{Mg} Ol = molar ratio of MgO/(MgO + FeO) of olivine; ND, not determined.

[b] Runs performed in Pt capsules that suffered variable amount of Fe loss.

[c] Runs performed in graphite sample containers welded into Pt capsules.

at 1550°C. Pressure calibration experiments were performed by means of the following phase transitions: quartz–coesite (3.2 GPa at 1200°C, Bose and Ganguly, 1995; fayalite-γ-Fe_2SiO_4, 5.0 GPa at 1000°C, Yagi et al., 1987; $CaGeO_3$ garnet–perovskite transition, 6.1 GPa at 1000°C, Susaki et al., 1985; coesite–stishovite, 9.2 GPa at 1200°C, Yagi and Akimoto, 1976; Zhang et al., 1996).

2.4. Analytical Technique

Alkali- and carbonate (CO_2)-rich experimental charges pose a particular challenge for preparation and analysis: The K-rich quenched liquids contain H_2O-soluble carbonates. All charges were embedded in epoxy resin and ground (without the use of water) to expose the longitudinal cross section. Intermittent impregnation with low viscosity epoxy resin under vacuum solved the problem of loosing parts of the fine grained charge, in particular the quenched liquid that is composed of a fine grained mixture of (alkali-) carbonates, silicates, and oxides. Final polishing with diamond powder was performed under petrol to avoid dissolution of the alkali carbonates. Charges were immediately coated with carbon coating and stored in a desiccator. All charges were analyzed with a Cameca SX50 microprobe with a PAP correction procedure (a modification of the ZAF corrections scheme) with 15 kV acceleration voltage and 10 (melts, i.e., fine-grained quench intergrowth and carbonates) and a 20-nA sample current. Beam diameters of 1 to 2 μm were used for silicate and carbonate phases and 10 to 50 μm for quenched melts.

3. RESULTS

3.1. Phase Equilibria of Group II Kimberlite from 1.5 to 10 GPa

The results of high-pressure experiments are listed in Table 2, and representative (average) melt and mineral compositions (garnet and pyroxenes) are listed in Table 3 (x_{Mg} olivine is listed in Table 2). The results of quenching experiments on the kimberlite composition (Table 1, A) are presented on Figure 1. The most prominent features of the phase diagram is that the group II kimberlite is multiply saturated with olivine–orthopyroxene–garnet (garnet harzburgite) over a wide P-T region; the liquidus was not encountered; even at 1480°C and 6 GPa or 1600°C and 9.5 GPa, run products comprised an estimated 15% of olivine + orthopyroxene + minor garnet crystals in a quench matrix. Phlogopite has a limited stability field, confined to low pressures and temperatures ($\leq$4.5 GPa and 1250°C) much less than its maximum thermal and pressure stability of 9 to 10 GPa/1400°C in simple systems (Luth, 1997; Sato et al., 1997) or in natural peridotite (Konzett and Ulmer, 1999). Outside the restricted stability field of phlogopite, no K-bearing silicate phase was found to be stable, even at the highest pressures and lowest temperatures. The restricted stability field

Table 3. Averaged pyroxene, garnet, and liquid compositions (wt)[a].

Run	P (GPa)	T (°C)	Phase	SiO_2	TiO_2	Cr_2O_3	Al_2O_3	FeO	MnO	MgO	CaO	Na_2O	K_2O	Total	x_{Mg}
470	2.0	1150	cpx	53.43	0.54	0.46	0.83	5.06	0.20	19.12	19.40	0.82	0.17	100.03	0.871
			Liquid	15.17	0.93	0.04	4.50	5.82	0.28	11.86	16.58	3.24	8.88	67.29	0.784
460	2.5	1200	cpx	53.01	0.36	0.41	3.25	6.17	0.23	18.19	16.64	1.38	0.20	99.85	0.840
474	2.5	1250	cpx	52.85	0.53	0.64	3.71	4.86	0.17	18.72	17.43	0.94	0.18	100.03	0.873
			cpx	56.34	0.26	0.55	2.30	6.94	0.20	32.63	2.24	0.19	0.06	101.69	0.893
			Liquid	26.19	2.00	0.16	6.28	5.73	0.20	13.84	13.17	1.94	7.71	77.22	0.811
471	3.0	1200	garnet	40.33	2.32	0.99	20.06	9.19	0.39	18.69	8.17	0.09	0.02	100.26	0.784
473	3.0	1250	opx	56.75	0.11	1.20	1.40	5.23	0.12	35.20	0.78	0.08	0.01	100.87	0.923
			Liquid	12.22	1.04	0.06	1.86	7.67	0.23	14.26	15.10	1.60	2.73	56.77	0.768
541	3.0	1300	opx	54.61	0.28	0.65	3.00	5.88	0.21	34.00	1.92	0.08	0.09	100.71	0.911
543	38	1150	opx	55.51	0.11	0.69	1.82	6.22	34.96	0.57	0.13	0.07	100.24	0.909	
540	3.8	1200	opx	55.47	0.64	0.29	2.76	7.55	0.21	32.57	1.25	0.08	0.10	0.00	0.885
			garnet	41.04	1.20	0.85	22.20	8.83	0.40	18.90	7.42	t0.03	0.07	0.00	0.792
547	4.0	1350	opx	57.56	0.09	0.65	2.56	2.82	0.11	36.81	0.59	0.11	0.02	101.31	0.959
			Liquid	34.16	1.15	0.25	5.48	4.39	0.21	24.32	7.15	1.30	4.25	82.67	0.908
MA27	4.6	1140	cpx	52.44	0.31	0.28	1.81	4.87	0.17	17.27	20.09	1.40	0.19	98.81	0.863
			opx	54.70	0.14	0.19	1.73	5.59	0.13	35.47	0.90	0.15	0.13	99.12	0.919
			garnet	41.08	0.96	0.91	19.17	10.37	0.33	21.94	5.60	0.05	0.06	100.46	0.790
			Liquid	8.01	2.18	0.07	1.20	7.96	0.21	19.29	15.89	2.63	10.67	68.09	0.812
MA26	4.6	1250	opx	56.20	0.10	0.37	2.20	5.89	0.16	33.92	0.82	0.12	0.09	99.86	0.911
			garnet	42.10	0.70	1.38	20.66	9.65	0.28	21.24	4.95	0.03	0.01	101.00	0.797
MA28	4.6	1400	opx	55.71	0.13	0.48	1.80	4.51	0.11	35.48	0.86	0.06	0.02	99.16	0.933
MA21	6.0	1250	opx	55.36	0.11	0.29	1.67	6.35	0.10	34.66	0.96	0.12	0.02	99.64	0.907
			garnet	40.94	0.95	1.50	20.23	8.56	0.27	22.38	4.28	0.04	0.05	99.20	0.823
			Liquid	13.08	2.78	0.12	3.38	7.69	0.22	19.34	12.05	0.63	4.99	64.29	0.818
MA20	6.0	1350	opx	55.38	0.18	0.19	1.10	6.05	0.18	34.03	1.32	0.18	0.16	98.76	0.909
			garnet	41.46	1.02	1.80	20.08	7.75	0.34	21.78	5.01	0.07	0.06	99.36	0.834
525	6.0	1400	opx	57.39	0.14	0.29	0.72	6.30	0.12	34.30	0.98	0.04	0.04	100.32	0.907
			garnet	42.39	0.82	3.00	20.71	6.07	0.27	22.02	5.54	0.04	0.07	100.92	0.866
548	6.0	1480	opx	57.16	0.13	0.37	1.31	5.84	0.21	34.83	0.85	0.17	0.09	100.96	0.914
			garnet	42.99	0.38	2.57	22.42	4.36	0.20	25.50	30.00	0.07	0.089	101.56	0.912
			Liquid	33.62	1.22	0.26	4.47	5.45	0.20	24.47	7.90	0.77	5.28	83.64	0.889
MA24	7.5	1150	cpx	53.68	0.14	0.36	0.51	3.43	0.1	19.30	21.15	0.46	0.09	99.32	0.909
			opx	55.98	0.15	0.17	0.44	8.17	0.13	34.25	0.56	0.06	0.05	100.06	0.882
			garnet	40.64	0.89	0.31	22.37	9.71	0.27	19.17	6.71	0.13	0.06	100.28	0.779
MA25	7.5	1200	cpx	53.76	0.17	0.26	0.66	4.08	0.19	18.98	20.49	0.59	0.10	99.28	0.892
			opx	56.67	0.13	0.21	0.59	7.30	0.18	33.90	0.90	0.10	0.01	99.99	0.892
			garnet	40.52	1.40	1.78	20.12	10.33	0.47	18.74	6.22	0.05	0.02	99.65	0.764
MA22	7.5	1280	opx	57.61	0.08	0.18	0.55	6.08	0.14	34.58	1.33	0.15	0.05	100.74	0.910
			garnet	42.51	0.78	1.98	20.28	7.53	0.29	21.85	5.15	0.04	0.07	100.49	0.838
MA23	7.5	1300	opx	56.52	0.08	0.22	0.50	5.51	0.12	35.04	0.93	0.14	0.06	99.28	0.919
			garnet	41.12	1.19	2.26	19.31	8.83	0.31	21.37	4.92	0.08	0.12	99.55	0.812
			Liquid	13.48	1.94	0.05	0.95	7.58	0.22	16.92	11.45	2.04	9.06	63.73	0.799
524	7.5	1450	opx	57.53	0.08	0.29	0.70	4.57	0.14	33.77	1.91	0.24	0.15	99.38	0.929
			garnet	43.62	1.07	2.31	19.72	5.76	0.24	23.39	5.05	0.09	0.13	101.36	0.879
642	8.0	1200	cpx	54.47	0.20	0.30	1.10	4.08	0.14	19.05	19.13	0.98	0.09	99.54	0.893
			opx	57.82	0.08	0.17	0.33	6.43	0.15	34.49	0.86	0.10	0.01	100.44	0.905
			garnet	41.52	1.77	2.02	18.50	10.93	0.35	19.61	5.48	0.11	0.01	100.29	0.762
646	8.0	1500	opx	58.10	0.10	0.19	0.76	5.29	0.13	34.68	0.99	0.16	0.01	100.39	0.921
			garnet	43.60	0.50	2.79	19.64	5.64	0.19	24.49	3.51	0.04	0.01	100.41	0.886
			Liquid	27.66	1.32	0.15	1.99	8.71	0.23	23.11	8.80	0.90	2.94	75.81	0.825
652	9.5	1200	cpx	54.39	0.61	0.14	0.96	6.40	0.19	16.94	18.28	1.62	0.30	99.82	0.825
			opx	56.47	0.08	0.18	0.28	7.63	0.13	34.12	0.46	0.13	0.03	99.49	0.888
			garnet	42.09	0.84	0.90	19.76	10.95	0.36	20.68	4.74	0.13	0.12	100.58	0.772
653	9.5	1400	opx	57.20	0.07	0.08	0.23	5.15	0.09	36.15	0.59	0.10	0.16	99.82	0.926
			garnet	41.82	1.60	2.88	17.44	8.66	0.32	20.91	5.91	0.09	0.03	99.66	0.811
655	9.5	1600	opx	56.33	0.07	0.15	0.59	5.18	0.13	36.04	1.56	0.19	0.03	100.28	0.925
			garnet	43.31	0.86	2.15	17.76	6.34	0.20	25.53	3.91	0.10	0.03	100.20	0.878

[a] A total of 3 to 10 analyses were averaged. x_{Mg} = molar ratio of MgO/(MgO + FeO), Fe as FeO. See Table 2 for run and phase abbreviations.

of phlogopite is most probably not just a function of reduced H_2O activity due to the presence of carbonate $-CO_2$: Wendlandt and Eggler (1980) have shown that the thermal stability of phlogopite is not strongly affected by the decrease of the H_2O activity in vapor-saturated experiments up to high x_{CO_2} approaching unity at 2.0 GPa. Nearly identical phase relations and stabilities limiting the occurrence of phlogopite have been observed by Sweeney (1994) in Na-rich and K-rich carbonatites, respectively.

Multiple saturation of the group II composition (Table 1, A) in lherzolitic phases occurs at ~3.0 GPa and 1250°C, but at much lower temperatures than the liquidus for this composi-

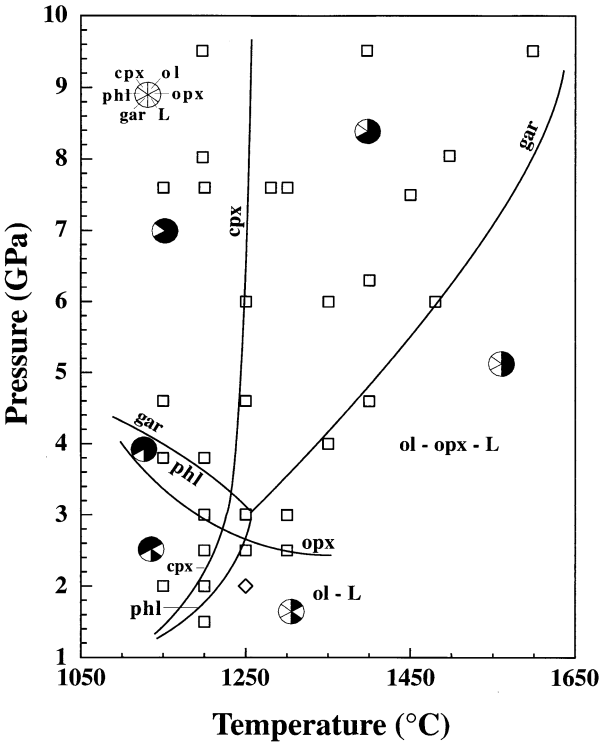

Fig. 1. Pressure–temperature (P in GPa and T in °C) diagram showing the experimental results of group II kimberlite melting experiments (bulk composition A in Table 1). The phase boundaries (solid lines) indicate the first occurrence of the phase labeled to lower temperatures, except for orthopyroxene and garnet that are labeled at the higher pressure side of the line. Above 6 GPa and below 1250°C, magnesite forms a stable phase together with ilmenite or TiO_2. Circles = assemblages present in the various regions of the phase diagram; solid sectors = phase present; void sectors = phases absent from paragenesis.

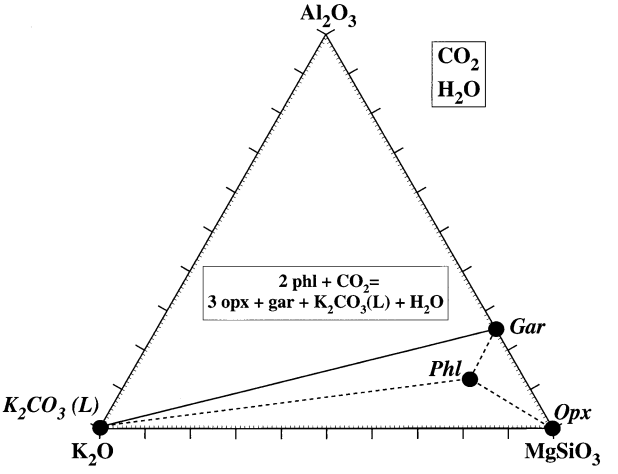

Fig. 2. Molecular diagram projected from CO_2 and H_2O onto K_2O-Al_2O_3-$MgSiO_3$ illustrating the phlogopite breakdown reaction at high pressures. The proposed breakdown reaction: 2 phlogopite + CO_2 = 3 enstatite + pyrope + K_2CO_3 (liquid) + H_2O. A similar reaction (disappearance of phlogopite coinciding with occurrence of garnet) was observed by Sweeney (1994) for potassic and sodic carbonatite compositions, respectively. At pressures higher than this breakdown reaction, no K-silicate phase was observed, even at the lowest temperatures of 900°C at 8 GPa.

tion. The liquids analyzed in experiments conducted at 2.5 to 3.0 GPa are significantly modified from a group II composition (Table 3) by olivine and orthopyroxene crystallization producing carbonatitic composition that bear little resemblance to a kimberlitic melt segregated at higher pressure. However, kimberlite melts that interact with lithospheric mantle at lower pressure may be modified to yield a similar composition. In general, multiple saturation with olivine + orthopyroxene + garnet ± clinopyroxene near the liquidus is regarded as prime requirement for a primary magma to be in equilibrium with a mantle residue of lherzolitic or harzburgitic composition. A kimberlitic primary melt may also (in addition to olivine and orthopyroxene) be saturated with a K-phase (phlogopite, K-richterite) and a CO_2-rich fluid or carbonate phase (mineral or melt). However, the concept of multiple saturation with mantle source constituents is only valid if no reaction relations between original source mineralogy and the product (incipient) melt occurs. In the case of CO_2-rich kimberlitic magmas, this is unlikely: The K-rich phase (phlogopite and/or K-richterite amphibole) exhibit incongruent melting on their own compositions (e.g., Yoder and Kushiro, 1969; Modreski and Boettcher, 1973; Konzett et al., 1997) producing K-rich melt/fluid and garnet-opx-olivine–bearing residues even in the absence of CO_2. Therefore, the absence of a K-rich phase close to the liquidus is not a proof of its absence in the mantle protolith, but it might have reacted out at near-solidus conditions. The inferred reaction destabilizing phlogopite in the kimberlite melt at 3 to 4 GPa is:

$$2\ \text{phlogopite} + CO_2 = 3\ \text{opx} + \text{garnet} + K_2CO_3\ (\text{L}) + 2\ H_2O\ (\text{L}) \quad (1)$$

(Fig. 2) and can also be formulated in the presence of a carbonate phase such as magnesite instead of CO_2 fluid (at pressure exceeding 4 GPa):

$$2\ \text{phlogopite} + MgCO_3 = 2\ \text{opx} + \text{olivine} + \text{garnet} + K_2CO_3\ (\text{L}) + 2\ H_2O\ (\text{L}). \quad (2)$$

Such a reaction relationship might be responsible for the phase assemblage observed in a low-temperature experiment conducted at 900°C and 8 GPa (run 561, Table 2) that contained garnet-cpx-opx-magnesite and OH clinohumite (at 8 GPa, OH-clinohumite is stable to ~1050°C in a hydrous peridotitic bulk composition, replacing olivine; Stalder and Ulmer, 2001) and a K-rich carbonatitic liquid (CaO/MgO ≈ 0.40) that quenched to fine intergrowth of K-Na-Ca-Mg carbonates. The low melting point of these alkali carbonates makes it unlikely that K-rich (hydrous) silicate phases coexists under ambient temperature conditions (even cold lithosphere) with such a K-Mg–rich carbonatite liquid at conditions >4 GPa. This is also the case in the carbonate-dominated bulk system (Sweeney, 1994). If group II kimberlites are indeed as CO_2-rich as published data (e.g., Mitchell, 1986, 1995) imply than they do not represent single-stage partial melts from carbonated (dolomite or magnesite bearing) phlogopite or K-richterite peridotite from within the diamond stability field.

The exceedingly high liquidus temperature of the studied group II kimberlite composition (>1500°C at 6 GPa and

>1600°C at 9.5 GPa) might indicate that kimberlite compositions, determined from bulk chemical analyses of extruded kimberlites, do not represent primary compositions, but are enriched in olivine, orthopyroxene, or garnet components, or some combination of these, as a result of incorporation of dismembered harzburgitic upper mantle xenoliths forming part of the macrocryst (pheno- or xenocrysts) assemblage characteristic for all but the most differentiated aphanitic kimberlites (e.g., Mitchell, 1995, 1997). In this case the primary liquid would be less Mg- (and probably also less Si-) rich than the inferred compositions—for example, the adjusted (Na_2CO_3 added) average group II composition of Smith et al. (1985) includes an overestimated amount of olivine/orthopyroxene. Alternatively, if mantle xenoliths incorporation has not been significant, group II kimberlite compositions represent liquid compositions, and it is most likely that such a liquid is in equilibrium with a garnet harzburgite residue (garnet is required from trace element considerations, (e.g., Tainton and McKenzie, 1994). The potassium would derive from phlogopite or potassium richterite above 6 GPa (Trønnes et al., 1988; Luth, 1997; Konzett and Ulmer, 1999); introduced in the original source assemblage by earlier metasomatism. The requirement of garnet in the residue constrains the group II kimberlite depth of origin to pressures >6 GPa where garnet stability approaches the liquidus (Fig. 1) and is consistent with occurrence of diamonds in group II kimberlites.

The presence of olivine as the most common phenocryst (or macrocryst) in kimberlitic magmas (e.g., Skinner and Clement, 1979; Clement et al., 1984) is consistent with the phase relations at elevated temperature for pressures < 2.5 GPa (Fig. 1). The reaction of garnet + orthopyroxene + K_2CO_3 + H_2O to phlogopite + CO_2 at low temperature and pressures (Fig. 2) is consistent with observations of the preferential assimilation of orthopyroxene and garnet by the host kimberlite magma (Clement, 1982; Shee, 1985; Skinner, 1989). Runs below 2.5 GPa and temperatures ≤1200°C exhibit a paragenesis of olivine + phlogopite + clinopyroxene in a fine-grained matrix consisting of quench phlogopite, calcite, olivine ± clinopyroxene. This assemblage corresponds to the typical phenocryst/microphenocryst association observed in macrocrystal group II kimberlites (orangeites): Abundant phlogopite with clinopyroxene in a fine-grained matrix of olivine, phlogopite and calcite. Monticellite, which is a typical groundmass to microphenocryst phase in group I (basaltic) kimberlites is absent in the present experiments. This change in low-pressure mineralogy is related to the distinctly higher abundances of K and Si in group II kimberlites compared with group I kimberlites.

3.2. Liquid and Mineral Compositions

Averaged mineral analyses along with some liquid compositions are reported in Table 3 and discussed in Figure 3).

3.2.1. Liquid Compositions

It was nearly impossible to obtain quantitative analyses from the quenched liquids even in charges that contained abundant liquid or the liquid separated into distinct layers at the top of the capsule. The melts never quenched to glass but consist of relatively coarse grained (10 to 50 μm) feathery, partly skeletal crystals that are formed by silicates and carbonates. In the stability field of phlogopite predominantly calcite–phlogopite–olivine with minor cpx forms the quench matrix; at high pressures (≥4 GPa) a K-(Na,Ca)-Mg–rich carbonates dominate the quench with minor olivine and opx. The compositions of the liquids were obtained with a defocused electron beam of 20 to 50 μm and 10 nA of sample current to decrease the alkali volatilization. Single points show large scatter and hence the averaged compositions have large standard deviations. The compositions indicated in Table 3 must be regarded as estimates of the true compositions. Nevertheless, the obtained liquid compositions show systematic variation with pressure (and temperature): Figure 3a shows the CaO/MgO variation as a function of pressure (and temperature). Liquids become increasingly MgO rich (decreasing CaO/MgO) with increasing pressure reflecting increasing amount of garnet and opx on the expense of olivine. High-temperature near-liquidus liquids at 4, 6, and 8 GPa plot on a trajectory toward the starting kimberlite composition. Low-temperature liquids in the range 1150 to 1300°C are carbonatitic with high alkali-contents and silica ranging mostly between 8 and 15 wt%.

3.2.2. Olivine

The Fe-Mg compositions of olivine are reported in Table 2 (last column) and illustrated in Figure 3b as a function of temperature. This relationship can be used to evaluate potential Fe loss to Pt capsules that had to been used in the initial stage of this study at temperatures exceeding 1300°C. Clearly, the experiments at 2 GPa/1200°C (in an AgPd capsule) and 4 GPa/1350°C suffered from considerable Fe loss, the remaining data set plots coherently. Of particular interest are the experiments at 7.5 and 8.0 GPa that have been performed with AgPd and Pt capsules (at 7.5 GPa) and graphite crucibles welded into Pt capsules (at 8 GPa), respectively: There is no systematic deviation of the x_{Mg} at 1450 and 1500°C with respect to the capsule material used. From this relationship we conclude that Fe loss is a problem in some of the runs, but that the majority of experiments were not seriously affected by the choice of container materials; phase equilibria are indistinguishable between the two sets of experiments at 7.5 to 8 GPa. The forsterite content of olivine (x_{Mg}) systematically decreases with increasing pressure at a given temperature. This effect is most probably due to increasing liquidus temperature that leads to higher crystallinity and hence differentiation (in terms of Fe-Mg) at a given temperature with increasing pressure.

High-Ca clinopyroxene (Figs. 3c and d) shows a systematic decrease of TiO_2 with increasing pressure. This decrease is accompanied by the occurrence of Fe-Ti oxides (ulvöspinel, ilmenite, TiO_2 [α-PbO_2 structure in excess of 7.5 GPa]) at low temperatures and high pressures—i.e., Ti is accommodated in oxide phases instead of silicate phases. A similar decrease of Ti contents is also observed in low-Ca pyroxene and garnet. This generally observed decrease of Ti solubility in pyroxenes with increasing pressure is most likely an effect of the decreasing Tschermak's component with increasing pressure and hence lack of charge balancing Al in the tetrahedral site of the pyroxenes. Cr_2O_3 decreases in both, high-Ca clinopyroxene (Fig. 3d) and low-Ca pyroxene (opx, not shown) with increasing pressure, most probably related to the occurrence of garnet

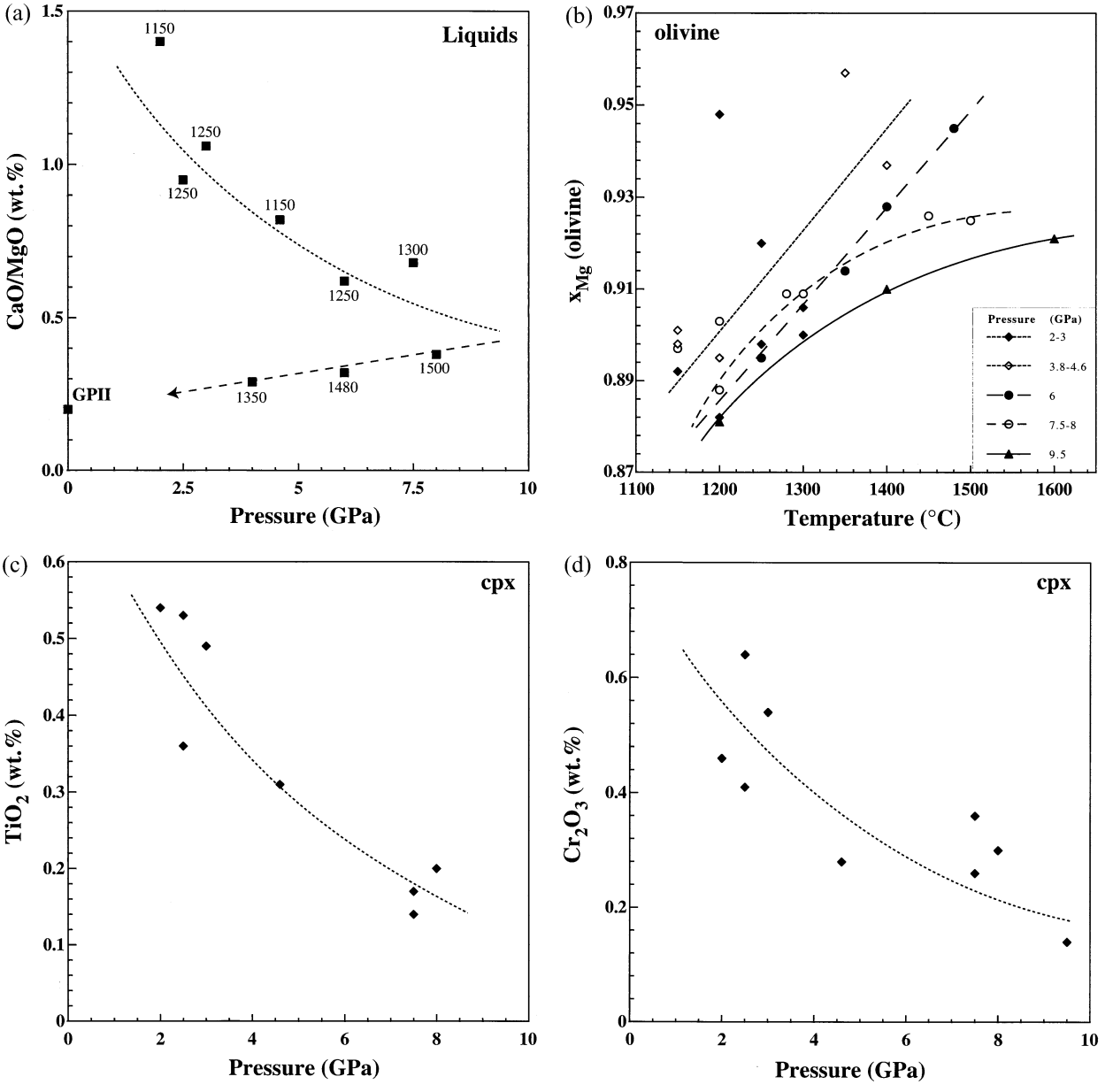

Fig. 3. Averaged (3 to 10 single analyses) liquid and mineral compositions as a functions of pressure and temperature of group II kimberlite experiments. (a) CaO/MgO (wt%) of liquids as a function of pressure, labels attached to data points indicate temperature of the experiment; (b) x_{Mg} (= molar MgO/(MgO + FeO)) of olivine as a function of temperature, different symbols and lines indicate various pressures (GPa); (c) TiO_2 (wt%) concentrations of clinopyroxene as a function of pressure; (d) Cr_2O_3 (wt%) concentrations of clinopyroxene as a function of pressure; (e) Al_2O_3 (wt%) content of orthopyroxene (low-Ca pyroxene) as a function of pressure; open diamonds = samples without coexisting garnet; filled diamonds = samples with coexisting garnet; (f) x_{Mg} (= molar MgO/(MgO + FeO)) of garnet as a function of temperature; different symbols and lines indicate various pressures (GPa); (g) Cr_2O_3 (wt%) concentrations of garnet as a function of pressure at temperatures in the range 1200 to 1250°C; (h) Cr_2O_3 (wt%) concentrations of garnet as a function of temperature at pressures in the range 7.5 to 8 GPa.

at pressures >3.0 GPa that accommodates most of the Cr and the decrease in Tschermak's component in pyroxenes with increasing pressure. K_2O is low in all high-Ca clinopyroxenes analyzed in this study and does exceed 0.30 wt% even at the highest pressure (9.5 GPa) and coexisting with a K-rich carbonatitic liquid.

Low-Ca pyroxene displays a systematic decrease of Al_2O_3 (Fig. 3e) for samples containing garnet, as expected from various experimental studies on Al distribution between garnet and low-Ca pyroxene (e.g., Wood and Banno, 1973; MacGregor, 1974; Brey et al., 1990). The Al-in-orthopyroxene geobarometer of Brey and Koehler (1990) (Fig. 4), by means of the experimental temperature as input, yielded consistent pressures up to the highest values (9.5 GPa) investigated. Most other published orthopyroxene–garnet geobarometers resulted in in-

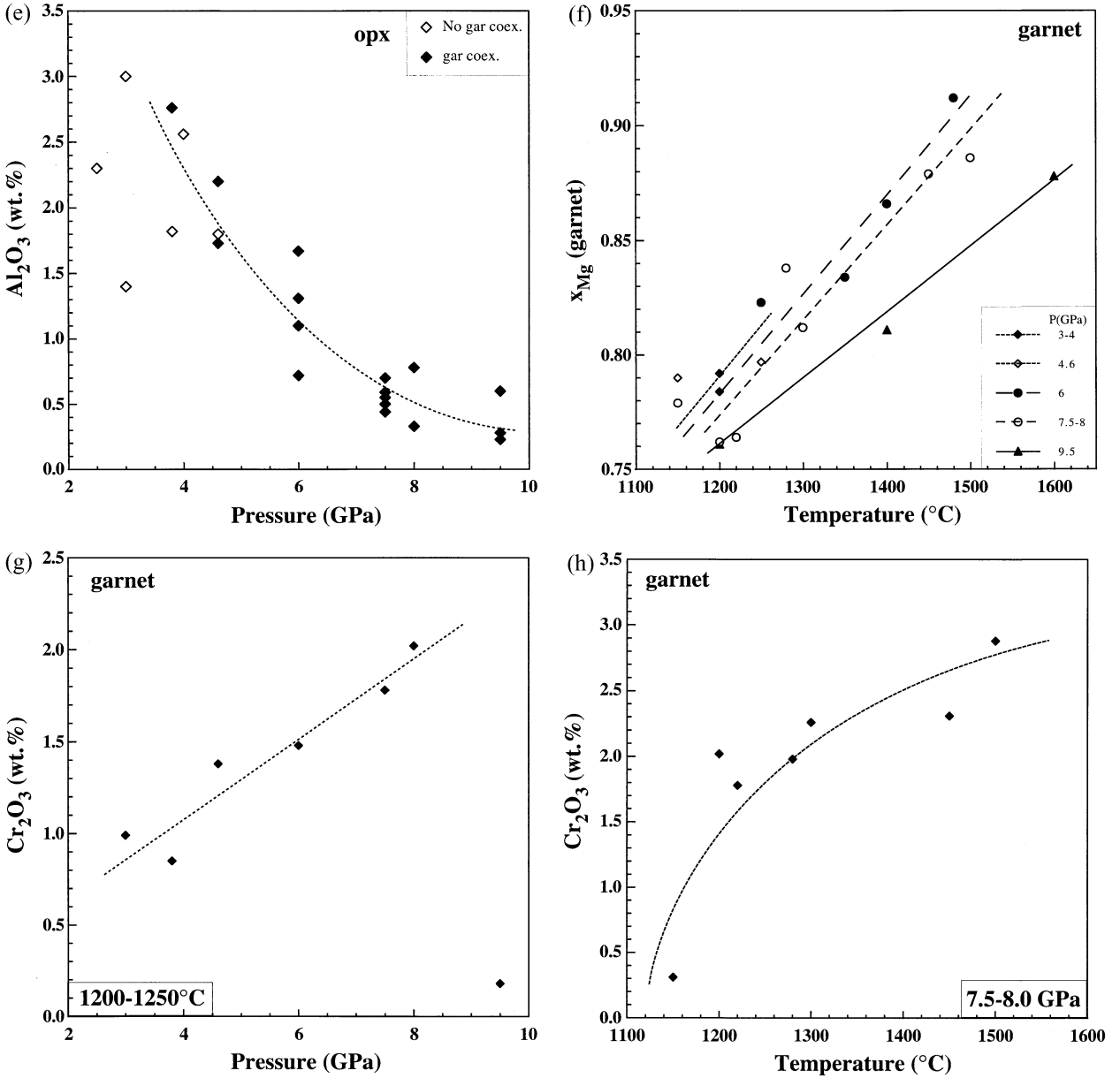

Fig. 3. Continued.

creasingly low calculated pressures with increasing pressures; at 9.5 GPa, most other barometers (e.g., Lane and Ganguly, 1980; Harley, 1984) yield pressures of 6 to 8 GPa, 2 to 3 GPa too low, whereas the expression by Bertrand et al. (1987) resulted pressures up to 15 GPa. The consistent results obtained with the orthopyroxene–garnet geobarometer of Brey and Koehler (1990) as well as the systematic variation of mineral compositions with pressure and temperature are indicative for close approach to chemical equilibrium during the experiment duration. Micro-Raman spectroscopy revealed that the low-Ca pyroxenes are orthopyroxenes (space group Pbca) up to pressures of 8 GPa and that the orthoenstatite–high-P clinoenstatite (space group C2/c) transition is crossed between 1400 and 1600°C at 9.5 GPa (for details, see Ulmer and Stalder, 2001).

Garnets show a systematic increase of Si with increasing pressure (and temperature). High temperature garnets (>1300°C) at pressures of >7.5 GPa consistently result Si >3.0 cations (based on 8 cations and 12 oxygens), indicating the presence of a majorite component (sixfold coordinated Si on the octahedral site). The Fe-Mg relationship of garnet is illustrated in Fig. 3f): similar to olivine, the x_{Mg} increases systematically as a function of temperature and pressure. With increasing pressure the x_{Mg} of garnets decrease for constant temperature reflecting increasing differentiation (crystallinity). Unlike the pyroxenes, Cr_2O_3 increases in garnet with both pressure and temperature (Figs. 3g and h) compensating for the decreased Cr solubility in the coexisting pyroxenes at high pressures.

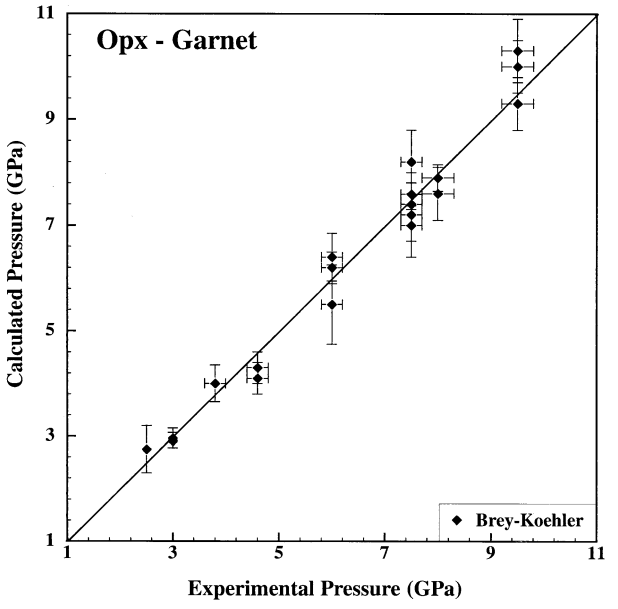

Fig. 4. Comparison of experimental pressures with pressures calculated from the orthopyroxene–garnet geobarometer of Brey and Koehler (1990). The two data points at 2.5 and 3.0 GPa are not from this study but rather from melting experiments on differentiated kimberlite compositions not discussed here. See text for discussion.

4. DISCUSSION

Eggler and Wendlandt (1979) examined the melting relations of an average Lesotho kimberlite (group Ia, Table 1) at 3 and 5.5 GPa. Solidus, liquidus, and phase relations are depicted in Fig. 5a. In this bulk composition at 5 GPa, a kimberlitic liquid is in equilibrium with olivine + orthopyroxene + clinopyroxene + garnet within 100°C of the liquidus. At 3 GPa, multiple saturation with these phases only occurs near the solidus of this bulk composition, which led to the conclusion that a kimberlitic composition cannot be primary at 3 GPa, but could be primary at 5.5 GPa. The solidus and liquidus position is consistent with observations in this study. The garnet-in boundary is also similarly located. However, the stability field for clinopyroxene is much expanded relative to this study (Figs. 5a and c) and no "backbend" was observed on the phlogopite-out curve. Eggler and Wendlandt (1979) used a composition that contained less CO_2 and a slightly lower x_{CO_2}, but possibly more important, their CO_2/SiO_2 ratio (CS, Table 1) is lower probably stabilizing diopside (cpx) to higher temperature. The increase in phlogopite pressure stability should not be dramatically affected by the CS ration as silica activity is buffered by the presence of olivine and opx in most experiments at high pressures.

Edgar et al. (1988) studied the phase relation of an aphanitic

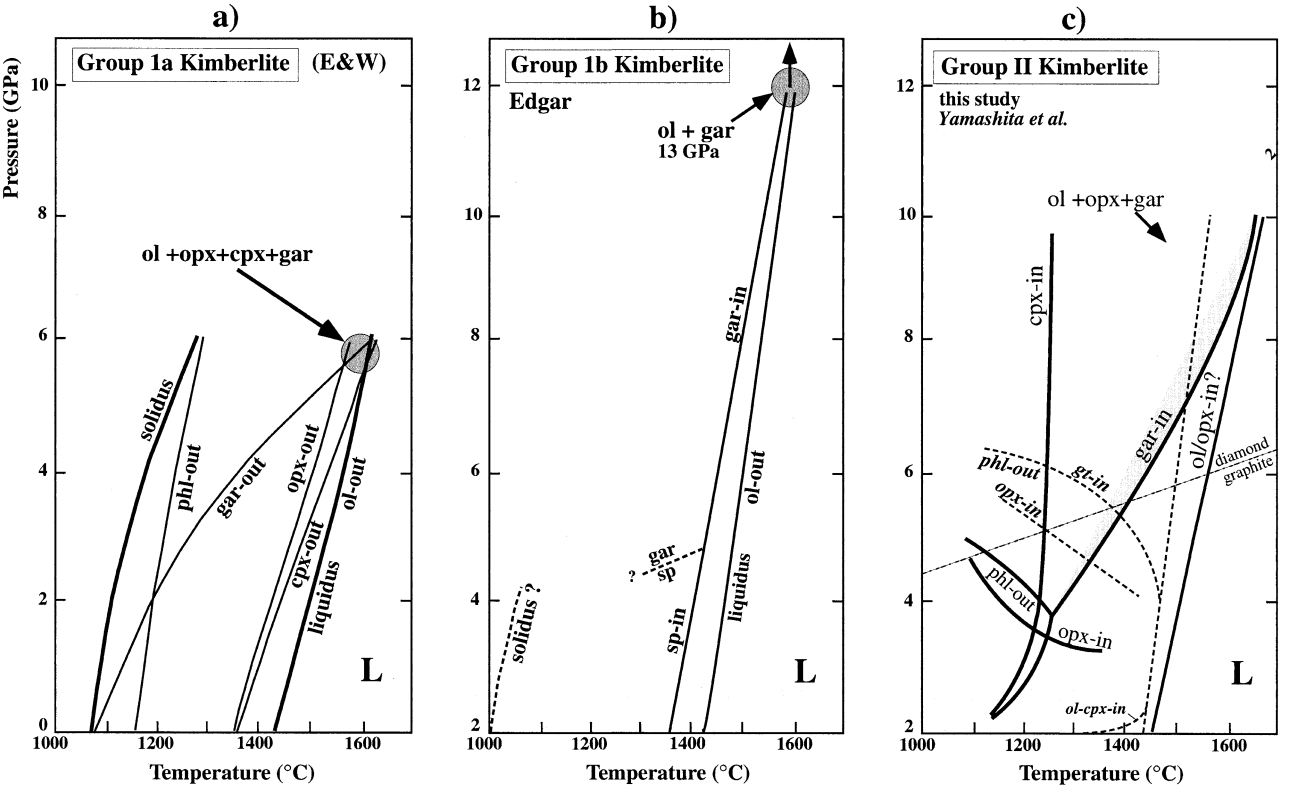

Fig. 5. Phase relations of experimental studies conducted on specific kimberlite bulk compositions. (a) Group Ia kimberlite (Eggler and Wendlandt, 1979) yielded multiple saturation (lherzolite) at ~6 GPa. The study by Girnis et al. (1995) found similar phase relations. (b) Group Ib (calcic) kimberlite composition (an aphanitic Wesselton kimberlite with 4.77 wt% CO_2) did not produce pyroxene as a liquidus phase (Edgar et al., 1988; Edgar and Charbonneau, 1993). (c) Group II (micaceous) kimberlite compositions (this study; solid lines and bold labels from Fig. 1), which saturates in a garnet harzburgite mineralogy near the liquidus (interpolated) over a considerable pressure interval (4 to 10 GPa). Dashed lines and labels in italics indicate the phase equilibria results from a study by Yamashita et al. (1995) on a similar composition that produced a considerably larger phlogopite stability field (see text for discussion).

group Ib kimberlite from Wesselton (Table 1) between 1 and 4 GPa, and Edgar and Charbonneau (1993) the same bulk composition between 5 and 10 GPa. In the lower pressure study two series of experiments were carried out: on the natural bulk composition (Edgar, Table 1), and the same composition with additional CO_2 (to total 10.34 wt%). At 3 GPa with 4.77 wt% total CO_2 (no added CO_2), the liquidus was located at 1430 ± 10°C with crystallization of olivine, olivine + spinel and olivine+ spinel + clinopyroxene down temperature (Fig. 5b). For the series with 10.34 wt% CO_2, the liquidus at 3 GPa was located at a higher temperature of 1465 ± 20°C and the liquidus assemblage was olivine + spinel, olivine + spinel + clinopyroxene down temperature. In no experiment was orthopyroxene or phlogopite observed as a crystallizing phase. The absence of orthopyroxene was explained by Edgar et al. (1988) as a consequence of the calcic nature of the bulk rock relative to group Ib kimberlites (Table 1) because the bulk composition lies on the calcic side of the olivine–clinopyroxene join in a projection (CMS) onto the base of the CMS-CO_2 system (Fig. 2; Edgar et al., 1988). At higher pressure (5 to 10 GPa, using the starting composition with 4.77 wt% CO_2), orthopyroxene was still absent (Fig. 5b), where at 7.5 GPa the assemblages olivine, olivine + garnet crystallize down temperature. No clinopyroxene was observed as a liquidus phase in the high-pressure study, which is consistent with the result of this study (Fig. 1). The absence of orthopyroxene as a near-liquidus phase contrasts with our results where it was ubiquitous at $P > 2.5$ GPa. We agree with Edgar et al. (1988) and Edgar and Charbonneau (1993), who state the absence of orthopyroxene is a result of the greater CaO and degree of silica undersaturation in their experiments (Table 1), even though CS (CO_2/SiO_2) is lower then in our experiments. These authors (op cit.) suggest that olivine stability at high pressure may be a function of low x_{CO_2} in the experiments (lowered by degassing of the natural rock) and that the Wesselton kimberlite and other low SiO_2, high CaO group Ib kimberlites may be derived from the partial melting of a carbonated garnetite (garnet ± clinopyroxene) present in the mantle as old subducted material (Ringwood, 1989). Alternatively, the Wesselton kimberlite represents a differentiate of a protokimberlitic magma derived from >10 GPa. We interpret the differences between the results presented in Fig. 5 as a function of the different bulk compositions used. For instance, the low SiO_2 of the group Ib kimberlite mitigates against the stability of pyroxenes at high P; therefore, saturation in only olivine and garnet occurs.

Girnis et al. (1995) investigated an average Lesotho group Ia (low alkali) kimberlite at 4.5 to 5.5 GPa as a function of variable bulk x_{CO_2} ranging from 0.31 to 1.0. No clinopyroxene stability was found, but at x_{CO_2} ranging from 0.31 to 0.71 olivine and orthopyroxene were liquidus phases joined by garnet in the pressure range 4.5 to 6 GPa with increasing x_{CO_2}. This study is similar to our results (the x_{CO_2} of the group II kimberlite starting material is 0.37, exactly in between the 0.45 and 0.34 chosen by Girnis et al. (1995) as their two lower starting compositions). Despite multiple saturation with olivine + orthopyroxene + garnet at 5 to 6 GPa, Girnis et al. (1995) favored the model proposed by Ringwood et al. (1992) and Kesson et al. (1994), i.e., formation of kimberlites in the transition zone (see below), because near liquidus garnets where unusually rich in Ti and poor Cr, unlike known garnet compositions from depleted upper mantle harzburgites. This bulk composition is similar to the group II kimberlite used in present study, with two significant differences: the group II composition has higher K_2O and lower MgO. The high K_2O in the group II composition ensures the stability of phlogopite at lower pressures and temperatures not explored by Girnis et al. (1995). Otherwise the two studies compare well, indicating that both kimberlite compositions may only be in equilibrium with a garnet harzburgite (clinopyroxene absent) mineralogy at liquidus conditions.

Ringwood et al. (1992) noted that rare earth element fractionation patterns in kimberlites imply that they were produced by partial melting in the presence of residual garnet. This is also indicated by the experimental results in Fig. 5, where all the assemblages marked as multiply saturated, include garnet. Ringwood et al. (1992) presented experiments on a synthetic group I kimberlite (Table 1), which showed that garnet (majorite) was present on the liquidus (with wadsleyite, or β-Mg_2SiO_4) at 16 GPa but well below the liquidus at 10 GPa. This supports a depth of origin of >300 km for their liquid (group Ia) composition. This is similar to the conclusion of that of Edgar and Charbonneau (1993) and Girnis et al. (1995) studies, although the bulk compositions (particularly CaO) are quite different.

Finally, there is one experimental study that is directly comparable to the present investigation: Yamashita et al. (1995) reported experimental phase relations on two different group II kimberlites from Makganyene Mine, South Africa in an extended abstract. In Fig. 5c), their results for the more primitive, macrocrystic group II kimberlite are reproduced, which have a comparable composition with the average group II kimberlite we have chosen, except for lower volatile contents and hence lower CO_2/SiO_2 (Table 1). The second composition investigated by Yamashita et al. (1995) was an aphanitic group II kimberlite that is differentiated (low MgO and H_2O, high K_2O, CaO, Al_2O_3, and CO_2) or crustally contaminated. Their phase relations are generally similar to the ones obtained in the present study, with the exception that phlogopite has a much larger stability field, representing the only liquidus phase at pressure up to 2 GPa joined by olivine and clinopyroxene at higher pressures. Phlogopite disappears at high pressures (4 to 6 GPa) in a similar fashion as observed in our experiments through a reaction forming garnet and orthopyroxene. The x_{CO_2} is nearly identical (0.351 as compared with 0.370 in our experiments) and should not be the reason for this discrepancy in phlogopite stability. The aphanitic kimberlite they investigated in addition, which has a x_{CO_2} of 0.586 and comparable amount of CO_2 as group II of this study (6.70 wt% as compared with 7.13 wt%) shows a similar, only slightly reduced, phlogopite stability field that exceeds 1400°C at 1 GPa and approaches 1500°C at 4 GPa. Comparing the stability of phlogopite in pure end-member systems reveals that the stability field inferred by Yamashita et al. (1995) exceeds the experimentally determined stability limits of phlogopite-opx (1120°C at 1 GPa, 1300°C at 3 GPa, Modreski and Boettcher, 1972; phlogopite-cpx, 1120°C at 1 GPa, 1300°C at 3.5 GPa, 1380°C at 6 GPa, Modreski and Boettcher, 1973; Luth, 1997) by 150 to 300°C. Even pure end-member OH-phlogopite has a considerably lower stability limit (1300°C at 1 GPa, 1380°C at 3 GPa, Yoder and Kushiro, 1969) than inferred by Yamashita et al. (1995). The only explanation we can come forward to explain the exceedingly high phlogopite stability in the experiments of Yamashita et al.

(1995) is the presence of considerable amount Fluorine in their starting material. Fluorine is known to stabilize phlogopite and other hydrous phases such as K-richterite amphibole to much higher temperatures. Kushiro et al. (1967) report F-phlogopite stable at 4 GPa and 1560°C; Foley et al. (1986) report phlogopite in a synthetic KMASF up to 1500°C at 2.8 GPa coexisting with olivine and enstatite. Unfortunately, Yamashita et al. (1995) do not report the Fluorine content of their starting materials or the phlogopites observed in their experiments. Our experiments were Fluorine free; the maximum thermal stability of phlogopite in the present experiments matches well the experimental data from Modreski and Boettcher (1972) and Luth (1997) on phlogopite-opx and phlogopite-cpx thermal stabilities of ~1250 to 1300°C at 3 GPa. Little is known about the Fluorine contents of group II kimberlites (orangeites); Mitchell (1995) reports generally low F-contents of phlogopite micas in group II kimberlites (≤1 wt%), mostly in the range 0.1 to 0.6 wt% and no bulk Fluorine of the analyzed group II kimberlites.

The experiments of Yamashita et al. (1995) would allow formation of group II kimberlites at ~4.5 GPa from a phlogopite–garnet peridotite. However, the presence of diamonds in most group II kimberlites and pressure determinations from garnet-bearing mantle xenoliths entrained in the group II kimberlites indicate pressures in excess of 6 GPa (Boyd, 1973; Carswell and Gibb, 1987), which argues against such low pressures of magma generation. In addition, both studies (and so far all multiple saturation experiments on "primary" kimberlites) failed to stabilize a carbonate phase (dolomite or magnesite) in the range of liquidus temperatures and therefore require that kimberlites are not formed at the carbonated peridotite solidus but at some temperature above where carbonate phases have been consumed. Alternatively, a two-stage process for the formation of carbonate-rich primary magmas from peridotitic sources in the stability region of diamond is required (see below).

Tainton and McKenzie (1994) examined the geochemistry of South African group II kimberlites and lamproites with the parameterization techniques of McKenzie and O'Nions (1991) and White et al. (1992). This study concluded that the composition of group II kimberlites might be produced from a source that has been extensively melted (17 to 26 wt%) in the garnet stability field and later enriched by a small melt fraction (4 to 10 wt%) produced from a MORB source by <0.5% melting. A constraint on the minimum depth of origin is found in the Cr number of garnet ($100 \times Cr/Cr + Al > 30$), which requires that garnet-bearing nodules entrained in kimberlite were in equilibrium with melt in the Cr-spinel stability field. To explain the influence of both garnet and spinel in kimberlite sources, Tainton and McKenzie (1994) invoke a two-stage model of depletion in the spinel stability field then lithospheric thickening to stabilize this protolith in the garnet stability field. This is consistent with the experimental results, which suggest a liquid of kimberlitic (group I or II) composition must derive from a depth >150 km (~5 GPa) where garnet is close to the liquidus. The maximum depth of 180 km derived by Tainton and McKenzie (1994) is dependent upon isotopic arguments; the group II compositions require source regions that have been isolated for at least 1 Ga, which indicates the lithospheric mantle. Thus, a derivation of group II kimberlites from 150 to 250 km would be consistent with isotopic, trace element and experimental data. We also point out that this conclusion is not inconsistent with the study of (Ringwood et al., 1992), as this deals with the origins of a group Ia kimberlitic liquid (~16 GPa). The deep derivation of group Ia kimberlites is consistent with some of the evidence for high P xenolithic data (Moore and Gurney, 1985; Haggerty and Sautte, 1990).

The above studies have dealt specifically with phase relations and geochemistry of kimberlitic bulk compositions. There is consensus amongst the models for kimberlite genesis, that they have at least equilibrated with peridotite-CO_2 and this system has been well-studied at $P < 4$ GPa (Mysen and Boettcher, 1975; Wyllie and Huang, 1975, 1976; Eggler, 1978; Wendtland and Mysen, 1980; Wyllie, 1980, 1987, 1989; Olafsson and Eggler, 1983; Taylor and Green, 1988; Wallace and Green, 1988; Falloon and Green, 1989; Moore and Wood, 1998; Lee et al., 2000; Lee and Wyllie, 2000). At pressures between 4 to 12 GPa, the phase relations of synthetic peridotites in CMS-CO_2, CMAS-CO_2, and CMS-CO_2-H_2O have been studied by Canil and Scarfe (1990) and Dalton and Presnall (1998a), (1998b). The solidus for CMAS-CO_2 and group II kimberlite phase relations (this study) suggests that a group II kimberlite may segregate from a garnet harzburgite at $P > 6$ GPa at T within ~100°C of the peridotite-CO_2 solidus (Dalton and Presnall, 1998b). The fact that kimberlites cannot be derived at pressures <3 GPa was also a conclusion of Eggler and Wendlandt (1979) and many others. Canil and Scarfe (1990) propose that group Ib (low SiO_2, high CaO) kimberlites derive from the mixing of carbonatitic and silicic (kimberlitic) melts at shallower depths. Canil and Scarfe (1990) and Dalton and Presnall (1998b) also showed that carbonates are the first phases consumed above the solidus, meaning that carbonates are unlikely to be residual in any kimberlite melting event. This is expected, considering the high solubility of carbonate in kimberlitic melts at $P > 4$ GPa (Brey et al., 1983, 1991). The proposed process is illustrated in Figure 6. A primary group II kimberlite is formed by carbonate–K-hydrosilicate–peridotite interaction and partial melting (defined by carbonate-phlogopite-(olivine)-opx on Fig. 6). Subsequent olivine–orthopyroxene–garnet fractionation (indicated by the dashed arrow) leads toward more alkaline- and carbonate-rich compositions that represent alkali–dolomitic carbonatites.

Why are K-Na-Mg-Ca–rich carbonatites never observed as magmas in the Earth's crust or preserved as mantle xenoliths? Many studies have shown that mantle carbonatites are ephemeral, above ~2 GPa. Phase equilibria studies on orthopyroxene-bearing carbonated peridotite systems (lherzolites or harzburgites), imperatively demonstrate that primary (Ca-Mg rich) carbonatitic liquids react with orthopyroxene at pressures of less than 2 to 3 GPa forming clinopyroxene + olivine + CO_2 fluid (Green and Wallace, 1988; Thibault et al., 1992; Dalton and Wood, 1993; Yaxley and Green, 1996; Wyllie and Lee, 1998; Lee et al., 2000; Lee and Wyllie, 2000). Petrographic evidence from mantle xenoliths entrained in kimberlites to alkali–olivine basalts clearly indicate that such metasomatic process linked to decarbonation of carbonatitic liquids are operating in the shallow part of the lithospheric mantle where they produce a spectrum of metasomatic features ranging from modal metasomatism evidenced by wehrlitic xenoliths to cryptic metasomatism identified in the trace element spectra of the

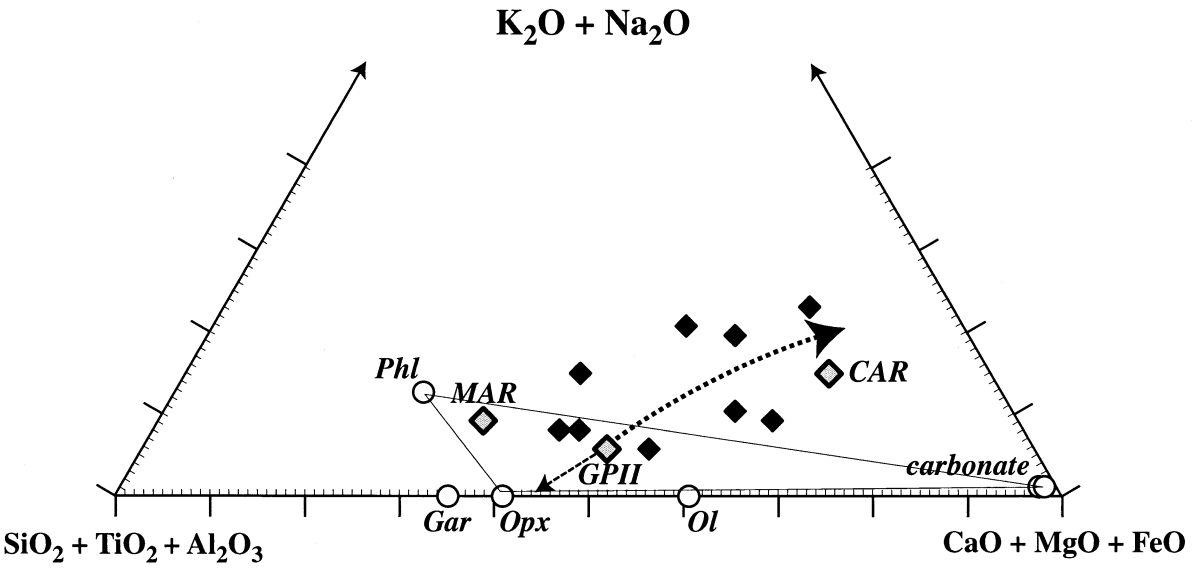

Fig. 6. Summary of liquid compositions obtained in the present study and comparison with mantle carbonatite composition obtained by Sweeney (1994). Pseudoternary (wt%) diagram after Freestone and Hamilton (1980) projected from CO_2 + H_2O. Open circles = composition of principal mineral phases in this system (using measured compositions); gray-filled diamonds = location of starting group II composition, MARID (MAR, AJE 137), and mantel carbonatite composition of Sweeney (1994) (CAR, S94); thick dashed curves = direction of differentiation of group II composition by olivine-opx-garnet fractionation to produce alkali–dolomitic–carbonatite derivative liquids. MARID compositions are not obtained by any combination of high-pressure cumulates of a group II composition.

minerals constituting the mantel xenoliths (e.g., Rudnick et al., 1993; Yaxley et al., 1998). Canil (1990) demonstrated that the decarbonation reactions in peridotitic mantle material proceed extremely fast, and inhibit the direct assent of carbonate bearing xenoliths from below the reaction boundary (2 to 3 GPa).

5. CONCLUSIONS

The group II bulk composition saturates in olivine + orthopyroxene + garnet over a considerable P-T range: from 3 to 10 GPa and 1300 to 1600°C. Clinopyroxene consistently appears on the liquidus at lower temperatures at ~1200 to 1250°C (3 to 10 GPa). The phlogopite–garnet transition in the silicate-dominated kimberlite bulk system is similar to that in the carbonate-dominated systems (Sweeney, 1994). The melt compositions in equilibrium with these assemblages are similar to the bulk starting composition and considered representative of a group II primary magma. Thus, group II kimberlites may be in equilibrium with a garnet harzburgite residue, which is phlogopite and clinopyroxene absent at liquidus conditions. However, as outlined in section 3.1, this does not exclude the presence of phlogopite (or K-richterite amphibole) in the protolith as it would incongruently melt at lower temperature to form an alkali–carbonate liquid. Phlogopite- and or K-richterite bearing (harzburgitic) peridotite compositions (phlogopite–peridotite, phlogopite–K-richterite–peridotite) are common in previously depleted lithospheric mantle, such as that represented by the Kaapvaal lithosphere, and group II kimberlitic melts show geochemical (isotopic) evidence for having interacted strongly with this lithosphere (Smith et al., 1985). Metasomatism by MARID-like liquids has been invoked to explain the K-enriched nature of many South African kimberlite-transported mantle xenoliths forming the succession from garnet–peridotite to phlogopite–peridotite to phlogopite–K-richterite–peridotite with increasing interaction with MARID-type liquids (Jones et al., 1982; Waters and Erlank, 1988; Jones, 1989). We propose that the occurrence of mantle-derived carbonatites and kimberlites are manifestations of similar processes in the Earth's mantle. Examination of carbonatite phase relations suggests that carbonatites result from the upward movement of volatiles or low viscosity melts (principally CO_2) from depth (Sweeney, 1994).

Examination of kimberlite solidus–liquidus relations imply that kimberlites would result from the interaction of volatiles (H_2O and CO_2) with a peridotitic mantle at higher temperatures than carbonatites and, critically, above the volatile-saturated peridotite solidus consistent with the results of Dalton and Presnall (1998b). For example, a carbonatite composition (Sweeney, 1994) may be 100% liquid at 4.6 GPa and 1150°C, whereas a kimberlite at the same pressure condition is near liquidus at 1450°C (this study, Fig. 1; Eggler and Wendlandt, 1979; Yamashita et al., 1995). Thus, a carbonatite melt may exist in a peridotitic mantle at the silicate sub or near-solidus condition, whereas a kimberlitic melt liquidus is clearly above the high pressure H_2O and high pressure H_2O-CO_2 solidii. A high-pressure experiment at low temperature (8 GPa, 900°C, run 561) indicates low solidus temperatures for alkali carbonatites, because all K and most of the Na are stored and concentrated in the liquid phase. This would imply that carbonatites in the presence of alkalis are always molten in the upper mantle at adiabatic temperature conditions.

The mutual exclusion of K-bearing (hydrous) silicates and carbonates/carbonatites (CO_2-rich fluids/melts) in the stability

field of diamonds points toward a multistage origin for group II kimberlites. Several scenarios fulfilling the minimum requirements can be envisaged. First, phlogopite or K-richterite occurring in cold peridotite (harzburgite, phlogopite–peridotite or phlogopite–K-richterite–peridotite) above a subducting slab or in cold regions of a subcratonic lithosphere is invaded by CO_2-rich fluids or melts (Konzett et al., 1997). This invasion leads to the immediate breakdown of the K-silicate–hydrate and to the formation of a group II kimberlitic magma in equilibrium with a garnet–harzburgite residue (Fig. 1).

Second, a carbonated (dolomite or magnesite bearing) peridotite is infiltrated by potassic hydrous fluids originating, for example, from the breakdown of phengitic white mica in subducted oceanic lithosphere (Schmidt, 1996). The presence of K-rich hydrous fluid or melt (probably supercritical) destabilizes the carbonate phase by dramatically lowering the solidus temperature in the peridotite and leads again to the formation of a group II kimberlite. For both processes, the destruction of phlogopite and generation of K-rich carbonatitic liquid will only occur at pressures greater than ~3.0 GPa because olivine + CO_2 are stable at lower pressures, and also phlogopite is stable at these conditions in equilibrium with a carbonate-rich melt (Sweeney, 1994; Yamashita et al., 1995; this study) or CO_2 (Eggler, 1978; Wyllie, 1978; Wendlandt and Eggler, 1980). Both processes require a first metasomatism event that either leads to the formation of a K-silicate–hydrate or a carbonate-bearing peridotite. The second-stage infiltration of either a carbonatite liquid or a K-rich hydrous fluid results in the production a K-rich kimberlitic liquid. Group II kimberlites, therefore, can only be produced in cold lithospheric mantle, which suffered multiple metasomatism events. The rare occurrence of group II kimberlite might be explained by the requirement that first, a cold lithosphere or subduction environment (to stabilize K-bearing phases) or K-metasomatism, and second, the presence of carbonate minerals or CO_2 as a fluid or melt have to interact at a common site.

Acknowledgments—We thank Bjorn Mysen for inviting the first author to participate in the symposium and in this volume. We are indebted to Jürgen Konzett and Alan Thompson for stimulating discussions, and we acknowledge Eric Reusser for assistance with microprobe analysis. We are grateful to Bob Luth and two anonymous reviewers for their critical and helpful comments. This study was financially supported by the Swiss National Science Foundation grant 20-61894.00.

Associate editor: D. B. Dingwell

REFERENCES

Bertrand P., Sotin C., Gaulier J. M., and Mercier J. C. C. (1987) La solubilite de l'aluminium dans l'orthopyroxene; inversion globale des donnees experimentales du systeme MgO-Al_2O_3-SiO2. *Bull. Soc. Geol. France. Huitieme Ser. 3* **5,** 821–832.

Bohlen S. R. and Boettcher A. L. (1982) The quartz–coesite transformation: A precise determination and the effects of other components. *J. Geophys. Res.* **87,** 7073–7078.

Bose K. and Ganguly J. (1995) Quartz–coesite transition revisited: Reversed experimental determinations at 500–1200°C and retrieved thermochemical properties. *Am. Mineral.* **80,** 231–238.

Boyd F. R. (1973) A pyroxene geotherm. *Geochim. Cosmochim. Acta* **37,** 2533–2546.

Brey G., Brice W. R., Ellis D. J., Green D. H., Harri K. L., and Ryabchikov I. D. (1983) Pyroxene–carbonate reactions in the upper mantle. *Earth Planet. Sci. Lett.* **62,** 63–74.

Brey G. P. and Koehler T. (1990) Geothermobarometry in four-phase lherzolites II. New thermobarometers, and pratical assessment of existing thermobarometers. *J. Petrol.* **31,** 1353–1378.

Brey G. P., Koehler T., and Nickel K. G. (1990) Geothermobarometry in four-phase lherzolites, I: Experimental results from 10 to 60 kbar. *J. Petrol.* **31,** 1313–1352.

Brey G., Kogarko L. N., and Ryabchikov I. D. (1991) Carbon dioxide solubility in kimberlitic melts. *N. Jb. Mineral. Monatshefte.* **1991,** 159–168.

Canil D. (1990) Experimental study bearing on the absence of carbonate in mantle-derived xenoliths. *Geology* 1011–1013.

Canil D. and Scarfe C. M. (1990) Phase relations in peridotite+ CO_2 systems to 12 GPa: Implications for the origin of kimberlites and carbonate stability in the Earth's upper mantle. *J. Geophys. Res.* **95,** 15805–15816.

Carswell D. A. and Gibb F. G. F. (1987) Garnet lherzolite xenoliths in the kimberlites of northern Lesotho: Revised P-T equilibration conditions and upper mantle Palaeogeotherm. *Contrib. Mineral. Petrol.* **97,** 473–487.

ClementC. R. (1982) A comparative geological study of some major kimberlite pipes in the Northern Cape and Orange Free State. Ph.D. thesis. University of Cape Town.

Clement C. R., Skinner E. M. W., and Scott-Smith B. H. (1984) Kimberlite redefined. *J. Geol.* **92,** 223–228.

Dalton J. A. and Presnall D. C. (1998a) Carbonatitic melts along the solidus of model lherzolite in the system CaO-MgO-Al_2O_3-SiO_2-CO_2 from 3 to 7 GPa. *Contrib. Mineral. Petrol.* **131,** 123–135.

Dalton J. A. and Presnall D. C. (1998b) The continuum of primary carbonatitic–kimberlitic melt compositions in equilibrium with lherzolite: Data from the system CaO-MgO-Al_2O_3-SiO_2-CO_2 at 6 GPa. *J. Petrol.* **39,** 1953–1964.

Dalton J. A. and Wood B. J. (1993) The composition of primary carbonate melts and their evolution through wallrock reaction in the mantle. *Earth Planet. Sci. Lett.* **119,** 511–525.

Dawson J. B. (1980) *Kimberlites and Their Xenoliths.* Springer-Verlag.

Dawson J. B. and Smith J. V. (1977) The MARID (mica–amphibole–rutile–ilmenite–diopside) suite of xenolith in kimberlites. *Geochim. Cosmochim. Acta* **41,** 309–323.

Edgar A. D., Arima M., Baldwin D. K., Bell D. R., Shee S. R., Skinner M. W., and Walker E. C. (1988) High-pressure–high-temperature melting experiments on a SiO_2-poor aphanitic kimberlite from the Wesselton mine, Kimberley, South Africa. *Am. Mineral.* **73,** 524–533.

Edgar A. D. and Charbonneau H. E. (1993) Melting experiments on a SiO_2-poor aphanitic kimberlite from 5–10 GPa and their bearing on source of kimberlite magmas. *Am. Mineral.* **78,** 132–142.

Eggler D. H. (1978) The effect of CO_2 upon partial melting of peridotite in the system Na_2O-CaO-Al_2O_3-MgO-SiO_2-CO_2 to 35 kb with an analysis of melting in a peridotite-H_2O-CO_2 system. *Am. J. Sci.* **278,** 305–343.

Eggler D. H. (1989) Kimberlites: How do they form?. In *Kimberlites and Related Rocks,* vol 1 (ed. J. Ross), p. 489–504. Blackwell.

Eggler D. H. and Wendlandt R. F. (1979) Experimental studies on the relationship of kimberlite magmas and partial melting of peridotite. In *Extended Abstracts, 2nd International Kimberlite Conference* (eds. F. R. Boyd and H. O. Meyer), p. 330–338. American Geophysical Union.

Falloon T. J. and Green D. H. (1989) The solidus of carbonated, fertile peridotite. *Earth Planet. Sci. Lett.* **94,** 364–370.

Foley S. F., Taylor W. R., and Green D. H. (1986) The effect of fluorine on phase relationships in the system $KAlSiO_4$-Mg_2SiO_4-SiO_2 at 28 kbar and the solution mechanism of fluorine in silicate melts. *Contrib. Mineral. Petrol.* **93,** 46–55.

Freestone I. C. and Hamilton D. L. (1980) The role of liquid immiscibility in the genesis of carbonatites—An experimental study. *Contrib. Mineral. Petrol.* **73,** 105–117.

Girnis A. V., Brey G. P., and Ryabchikov I. D. (1995) Origin of group IA kimberlites: Fluid-saturated melting experiments at 45–55 kbar. *Earth Planet. Sci. Lett.* **134,** 283–296.

Green D. H., Falloon T. J., and Taylor W. R. (1987) Mantle-derived magmas—Roles of variable source peridotite and variable C-H-O fluid compositions. In *Magmatic Processes: Physiochemical principles,* vol 1 (ed. B. O. Mysen), pp. 139–154. Geochemical Society.

Green D. H. and Wallace M. E. (1988) Mantle metasomatism by ephemeral carbonatite melts. *Nature* **336,** 459–462.

Haggerty S. E. and Sautte V. (1990) Ultradeep (greater than 300 km), ultramafic upper mantle xenoliths. *Science* **248,** 993–996.

Harley S. L. (1984) The solubility of alumina in orthopyroxene coexisting with garnet in FeO-MgO-Al_2O_3-SiO_2 and CaO-FeO-MgO-Al_2O_3-SiO_2. *J. Petrol.* **25,** 665–696.

Jones A. P. (1989) Upper mantle enrichment by kimberlitic or carbonatitic magmatism. In *Carbonatites: Genesis and evolution* (ed. K. Bell), pp. 448–463. Unwin Hyman.

Jones A. P., Smith J. V., and Dawson J. B. (1982) Mantle metasomatism in 14 veined peridotites from Bultfontain Mine, South Africa. *J. Geol.* **90,** 435–453.

Kesson S. E., Ringwood A. E., and Hibberson W. O. (1994) Kimberlite melting relations revisited. *Earth Planet. Sci. Lett.* **121,** 261–262.

Konzett J., Sweeney R. J., Thompson A. B., and Ulmer P. (1997) Potassium amphibole stability in the upper mantle: An experimental study in a peralkaline KNCMASH system to 8.5 GPa. *J. Petrol.* **38,** 537–568.

Konzett J., Armstrong R. A., and Sweeney R. J. W. C. (1998) The timing of MARID metasomatism in the Kaapvaal mantle: An ion probe study of zircons from MARID xenoliths. *Earth Planet. Sci. Lett.* **160,** 133–145.

Konzett J. and Ulmer P. (1999) The stability of hydrous potassic phases stability in lherzolitic mantle—An experimental study to 9.5 GPa in simplified and natural bulk compositions. *J. Petrol.* **40,** 629–652.

Kushiro I., Syono Y., and Akimoto S. (1967) Stability of phlogopite at high pressures and possible presence of phlogopite in the Earth's upper mantle. *Earth Planet. Sci. Lett.* **3,** 197–203.

Lane D. L. and Ganguly J. (1980) Al_2O_3 solubility in opx in the system MgO-Al_2O_3-SiO_2: A reevaluation and mantle geotherms. *J. Geophys. Res.* **85,** 6963–6972.

Lee W.-J., Huang W. L., and Wyllie P. J. (2000) Melts in the mantle modeled in the system CaO-MgO-SiO_2-CO_2 at 2.7 GPa. *Contrib. Mineral. Petrol.* **138,** 199–213.

Lee W.-J. and Wyllie P. J. (2000) The system CaO-MgO-SiO_2-CO_2 at 1 GPa, metasomatic wehrlites, and primary carbonatite magmas. *Contrib. Mineral. Petrol.* **138,** 214–228.

Luth R. W. (1997) Experimental study of the system phlogopite-diopside from 3.5 to 17 GPa. *Am. Mineral.* **82,** 1198–1209.

MacGregor I. (1974) The system MgO-Al_2O_3-SiO_2. Solubility of Al_2O_3 in enstatite for spinel and garnet peridotite compositions. *Am. Mineral.* **59,** 110–119.

McKenzie D. and O'Nions R. K. (1991) Partial melt distributions from inversion of rare earth element concentrations. *J. Petrol.* **32,** 625–679.

Mitchell R. H. (1986) *Kimberlites: Mineralogy, geochemistry, and petrology*. Plenum Press.

Mitchell R. H. (1995) *Kimberlites, orangeites, and related rocks*. Plenum Press.

Mitchell R. H. (1997) *Kimberlites, orangeites, lamproites, melilitites, and minettes: A petrographic atlas*. Kromar.

Modreski P. J. and Boettcher A. L. (1972) The stability of phlogopite + enstatite at high pressures: A model for micas in the interior of the Earth. *Am. J. Sci.* **272,** 852–869.

Modreski P. J. and Boettcher A. L. (1973) Phase relationships of phlogopite in the system K_2O-MgO-CaO-Al_2O_3-SiO_2-H_2O to 35 kilobars: A better model for micas in the interior of the Earth. *Am. J. Sci.* **273,** 385–414.

Moore R. O. and Gurney J. J. (1985) Pyroxene solid-solution in garnets included in diamond. *Nature* **318,** 553–555.

Moore K. R. and Wood B. J. (1998) The transition from carbonate to silicate melts in the CaO-MgO-SiO_2-CO_2 system. *J. Petrol.* **39,** 1943–1951.

Mysen B. O. and Boettcher A. L. (1975) Melting of hydrous mantle. I. Phase relations of natural peridotite at high P and T and with controlled addition of water, carbon dioxide and hydrogen. *J. Petrol.* **16,** 520–548.

Olafsson M. and Eggler D. H. (1983) Phase relations of amphibole, amphibole–carbonate, and phlogopite–carbonate peridotite: Petrologic constraints on the asthenosphere. *Earth Planet. Sci. Lett.* **64,** 305–315.

Ringwood A. E. (1989) Composition and evolution of the mantle. In *Kimberlites and Related Rocks* (ed. J. Ross), pp. 457–485. Blackwell.

Ringwood A. E., Kesson S. E., Hibberson W., and Ware N. (1992) Origin of kimberlites and related magmas. *Earth Planet. Sci. Lett.* **113,** 521–538.

Rudnick R. L., McDonough W. F., and Chappell B. W. (1993) Carbonatite metasomatism in the northern Tanzanian mantle: Petrographic and geochemical characteristics. *Earth Planet. Sci. Lett.* **114,** 463–475.

Sato K., Katsura T., and Ito E. (1997) Phase relations of natural phlogopite with and without enstatite up to 8 GPa: Implications for mantle metasomatism. *Earth Planet. Sci. Lett.* **146,** 511–526.

Schmidt M. W. (1996) Experimental constraints on recycling of potassium from subducted oceanic crust. *Science* **272,** 1927–1930.

SheeS. R. (1985) The petrogenesis of the Wesselton mine kimberlites, Kimberley, Cape Province, RSA. Ph.D. thesis. University of Cape Town.

Skinner E. M. W. (1989) Contrasting group I and group II kimberlite petrology: Toward a genetic model for kimberlites and related magmas. In *Kimberlites and related rocks* (ed. J. Ross), pp. 528–544. Blackwell.

Skinner E. M. W. and Clement C. R. (1979) Mineralogical classification of southern African kimberlites. In *Kimberlites, diatremes and diamonds: Their geology, petrology and geochemistry* (eds. F. R. Boyd and H. O. Meyer), pp. 129–139. American Geophysical Union.

Smith C. B., Gurney J. J., Barton E. S., and Bristow J. W. (1985) Geochemical character of southern African kimberlites: A new approach based on isotopic constraints. *Trans. Geol. Soc. South Africa* **88,** 267–280.

Stalder R. and Ulmer P. (2001) Phase relations of a serpentine composition between 5 and 14 GPa—Significance of clinohumite and phase E as water carriers into the transition zone. *Contrib. Mineral. Petrol.* **140,** 670–679.

Susaki J., Akaogi M., Akimoto S., and Shiomura O. (1985) Garnet–perovskite transormation in $CaGeO_3$: In-situ X-ray measurements using synchrotron radiation. *Geophys. Res. Lett.* **12,** 729–732.

Sweeney R. J. (1994) Carbonatite melt compositions in the Earth's mantle. *Earth Planet. Sci. Lett.* **128,** 259–270.

Sweeney R. J., Thompson A. B., and Ulmer P. (1993) Phase relations of natural MARID composition and implications for MARID genesis, lithospheric melting and mantle metasomatism. *Contrib. Mineral. Petrol.* **115,** 225–241.

Tainton K. M. and McKenzie D. (1994) The generation of kimberlites, lamproites, and their source rocks. *J. Petrol.* **35,** 787–817.

Taylor W. R. and Green D. H. (1988) Measurement of reduced peridotite-C-O-H solidus and implications for redox melting of the mantle. *Nature* **332,** 349–352.

Thibault Y., Edgar A. D., and Lloyd F. E. (1992) Experimental investigation of melts from a carbonated phlogopite lherzolite: Implications for metasomatism in the continental mantle. *Am. Mineral.* **77,** 784–794.

Trønnes R. G., Takahashi E., and Scarfe C. M. (1988) Stability of K-richterite and phlogopite to 14 GPa. *EOS Trans. Am. Geophys. Union* **69,** 1510–1511.

Ulmer P. and Stalder R. (2001) The Mg(Fe)SiO_3 orthoenstatite–clinoenstatite transitions at high pressures and temperatures determined by Raman-spectroscopy on quenched samples. *Am. Mineral.* **86,** 1267–1274.

Walker D. (1991) Lubrication, gasketing, and precision in multianvil experiment. *Am. Mineral.* **76,** 1092–1100.

Walker D., Carpenter M. A., and Hitch C. M. (1990) Some simplification to multianvil devices for high pressure experiments. *Am. Mineral.* **75,** 1010–1028.

Wallace M. E. and Green D. H. (1988) An experimental determination of primary carbonatite magma composition. *Nature* **335,** 343–346.

Waters F. G. and Erlank A. J. (1988) Assessment of the vertical extent and distribution of mantle metasomatism below Kimberley, South Africa. In *Journal of Petrology, Oceanic and continental lithospheric similarities and differences.* (ed. M. A. Menzies and K. G. Cox), pp. 185–204. Clarendon Press.

Wendlandt R. F. and Eggler D. H. (1980) The origin of potassic magmas, 2: Stability if phlogopite in natural spinel lherzolite and in the system $KAlSiO_4$-MgO-SiO_2-H_2O-CO_2 at high pressures and high temperatures. *Am. J. Sci.* **280,** 421–458.

Wendtland R. F. and Mysen B. O. (1980) Melting phase relations of natural peridotite + CO_2 as a function of degree of partial melting at 15 and 30 kbar. *Am. Mineral.* **65,** 37–44.

White R. S., McKenzie D., and O'Nions R. K. (1992) Oceanic crustal thickness from seismic measurements and rare earth element inversions. *J. Geophys. Res.* **97,** 19683–19715.

Wood B. J. and Banno S. (1973) Garnet-opx and opx-cpx relations in simple and complex systems. *Contrib. Mineral. Petrol.* **42,** 109–124.

Wyllie P. J. (1978) Mantle fluid compositions buffered in peridotite-CO_2-H_2O by carbonates, amphiboles and phlogopite. *J. Geol.* **86,** 687–713.

Wyllie P. J. (1980) The origin of kimberlite . *J. Geophys. Res.* **85,** 6902–6910.

Wyllie P. J. (1987) Discussion of recent papers on carbonated peridotite, bearing on mantle metasomatism and magmatism. *Earth Planet. Sci. Lett.* **82,** 391–397.

Wyllie P. J.The genesis of kimberlites and some low-SiO_2, high alkali magmas: Geological Society of Australia Special Publication 14. In *Kimberlites and Related Rocks* (ed. J. Ross), pp. 603–615. Blackwell.

Wyllie P. J. (1994) Experimental petrology of upper mantle materials, processes and products. In *Journal of Geodynamics, Proceedings of the International Symposium on the physics and chemistry of the upper mantle (ISUM)* (ed. F. B. Ribeiro), pp. 429–468. Pergamon Press.

Wyllie P. J. and Huang W. L. (1975) Peridotite, kimberlite and carbonatite explained in the system CaO-MgO-SiO_2-CO_2. *Geology* **3,** 621–624.

Wyllie P. J. and Huang W. L. (1976) Carbonation and melting reactions in the system CaO-MgO-SiO_2-CO_2 at mantle pressures with geophysical and petrological applications. *Contrib. Mineral. Petrol.* **54,** 79–107.

Wyllie P. J. and Lee W.-J. (1998) Model system controls on conditions for formation of magnesiocarbonatite and calciocarbonatite magmas from the mantle. *J. Petrol.* **39,** 1885–1893.

Yagi T. and Akimoto S.-I. (1976) Direct determination of coesite-stishovite transition by in-situ X-ray measurements. *Tectonophysics* **35,** 259–270.

Yagi T., Akaogi M., Shimomura O., Suzuki T., and Akimoto S.-I. (1987) In situ observation of the olivine–spinel phase transition in Fe_2SiO_4 using synchrotron. *J. Geophys. Res.* **92(B7),** 6207–6213.

Yamashita H., Arima M., and Ohtani E. (1995) High pressure melting experiments on group II kimberlite up to 8 GPa; implications for mantle metasomatism. Proceedings of the international Kimberlite conference. **6,** 669–671.

Yaxley G. M. and Green D. H. (1996) Experimental reconstruction of sodic dolomitic carbonatite melts from metasomatised lithosphere. *Contrib. Mineral. Petrol.* **124,** 359–369.

Yaxley G. M., Green D. H., and Kamenetsky V. (1998) Carbonatite metasomatism in the southeastern Australian lithosphere. *J. Petrol.* **39,** 1917–1930.

Yoder H. S. and Kushiro I (1969) Melting of a hydrous phase: Phlogopite. *Am. J. Sci.* **267A,** 558–582.

Zhang J., Utsumi W., and Liebermann R. C. (1996) In situ X-ray observations of the coesite–stishovite transition: Reversed phase boundary and kinetics. *Phys. Chem. Mineral.* **23,** 1–10.